Attorney's Docket No. P04-01 **PATENT APPLICATION**

IN THE UNITED STATES PATENT AND TRADEMARK OFFICE

In re application of: Fairchild

Serial No.: 10/711,593 **Group No.:** 3641

Filed: September 28, 2004 **Examiner:** Lee, Benjamin P.

For: FLIGHT CONTROL METHOD AND APPARATUS TO PRODUCE INDUCED YAW

Commissioner for Patents
P.O. Box 1450
Alexandria, VA 22313-1450

DECLARATION UNDER 37 CFR 1.132

Dear Sir:

I, Mark David Fairchild of 358 Main St. Apt. 4, Royersford, PA 19468, declare that:

I hold the degree of BS Aerospace Engineering from the University of Arizona (2000) and the degree of MS Aerospace Engineering from Penn State University (2003).

I have worked in the aerospace industry for eight years.

I am currently employed at Science Applications International Corporation of 1150 First Ave. STE 400, King of Prussia, PA 19406. My title is AEROSPACE ENGINEER. My experience includes aerodynamic modeling, vehicle 6DoF trajectory simulation and flight performance analysis, and aerothermal analysis. My flight test support activities involve pre-test range safety analyses and post-test flight data analysis, reduction, and documentation. I have been involved with multiple supersonic wind tunnel test entries; providing support for test planning, on-site testing, and post-test data analysis and report documentation.

I am a named inventor in the above-identified patent application and attached is an analysis that shows the Richard et al. reference used by the Examiner can not produce induced yaw as claimed in the claims of the above-identified patent application.

I further declare that all statements made herein of my own knowledge are true and that all statements made on information and belief are believed to be true; and that these statements were made with the knowledge that willful false statements and the like so made are punishable by fine or imprisonment, or both, under Section 1001 of Title 18 of the United States Code, and that such willful false statements may jeopardize the validity of the application or any patents issuing thereon.

Dec. 24, 2007
Date

Mark David Fairchild

FLIGHT CONTROL METHOD AND APPARATUS TO PRODUCE INDUCED YAW

Induced Drag Analysis of "Wing-Tip Control Surface For Aircraft" 2565990 Richard et. al

By

Mark Fairchild

December 26, 2007

Abstract

An aerodynamic analysis was performed to quantify the induced drag producing characteristics of the endplates described by Richard in his design. Only aerodynamic factors that contribute to downwash and induced drag were investigated, to isolate the induced drag generated by a given endplate deflection. Using established aerodynamic methods and principles, an induced drag solution was found that agrees with known induced drag results for selected endplate planforms. It has been shown that for every hinge deflection combination of Richard's endplates shown in his design, the resultant induced drag combination will only produce adverse yaw to the turn. Thus Richard's design is incapable of producing Induced Yaw to the turn in any measure and can only produce an induced drag differential that creates additional adverse yaw, rather than overcoming it.

Introduction

The purpose of this analysis is to show the induced drag effects that occur when Richard's endplate control surfaces are deflected, the type of contribution it makes to yawing a plane through a turn, and how it relates to both the applicant's design and examiner's comments. The nature of the aerodynamic analysis will be confined to only the factors that influence the production of induced drag for a given wing-endplate configuration, ignoring all other forms of drag and yaw. As it is the amount of induced flow generated by each wing half, and the balance between them, which determines if the yawing moment created is in the direction of the turn.

To illustrate the direction of the analysis we look at the classical equation for induced drag is:

$$\mathbf{C_{Di} = C_L^2/(\pi * Ae)}$$

Where $\mathbf{C_{Di}}$ is the Induced Drag Coefficient, $\mathbf{C_L}$ is the wing total lift coefficient, and **Ae** is the wing effective aspect ratio. This equation demonstrates that induced drag is solely the function of the wing lift coefficient and the wing aspect ratio, and by extension Induced Yaw is also the function of these properties. The analysis covers all factors that contribute to the total lift of the wing $\mathbf{C_L}$ and wingspan efficiency **e** that are a function of endplate deflection. It is the intent of this dissertation to itemize all contributing factors to wing lift and span efficiency, provide explanation of their known effects, and combine all relevant factors in a classical aerodynamic solution illustrating the induced drag produced as a function of endplate deflection and it ability to produce yaw.

It is also important to reiterate the limitation on the method of Induced Yaw. Quoting claim 1 of the applicant's patent:

> 1. (currently amended) A method of controlling an aircraft in a turn without the use of ~~a~~ rudder <u>control</u> by producing induced yaw, comprising: creating a net induced drag differential between an inboard wing to the turn and an outboard wing to the turn, the net induced drag differential being created in such a manner that the net induced differential overcomes adverse yaw produced by the outboard wing.

The limitation on Induced Yaw is that an induced drag differential is created such that the net balance of the differential is in the direction of the turn. The outboard wing to the turn is by definition, the one with the greater lift. To paraphrase claim 1:

For Induced Yaw to exist as a method of control, the wing which produces more lift must also generate less induced drag than the opposite wing.

This is the criteria which will determine whether or not Richard's design uses Induced Yaw as a method of flight control.

SECTION 1
Notes on Richard's Design

A brief explanation of how the analysis nomenclature applies to Richard's design.

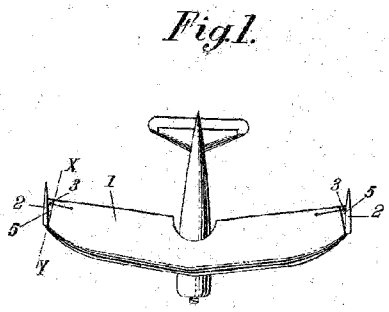

Figure 1. Design of Richard et al Aircraft Control Device

Endplate Deflection Angle Definition: The endplates rotate about an axis X-Y as shown in Fig. 1 of Richard's patent. The applicant has defined a deflection angle α_H to be the rotation of a given endplate out of the neutral position. The limits on hinge deflection are $-90 < \alpha_H < +90$ where a positive value denotes a lowering of the endplate below the wing (right side of Fig. 2) and a negative value for hinge angle denotes a raising of the endplate (left side of Fig. 2). In this manner positive hinge deflections correspond to an increase in wing lift, and negative deflections correspond to a decrease in lift.

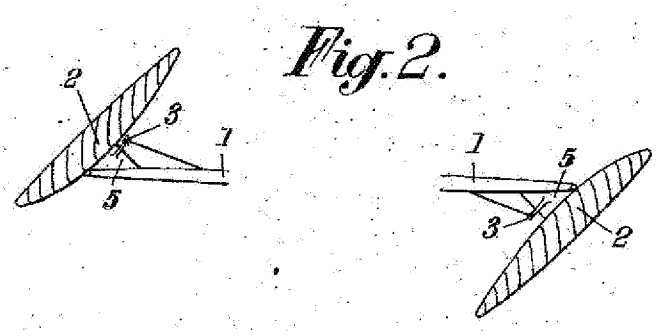

($\alpha_H < 0$; Lift Decrease) **($\alpha_H > 0$; Lift Increase)**

Figure 2. Endplate Deflection Detail

All plots will reference this hinge angle nomenclature.

Background: Induced Flow, Adverse Yaw, Endplates, and Winglets

It is worth noting some of the relevant properties of induced flow, and the devices used to counteract it, as all will be seen in Richard's design.

Induced Flow: To review, induced drag constitutes the drag effects that occur when a 3 dimensional wing with a pressure differential between the top and bottom surfaces, experiences flow "leakage" about the wingtips as the pressure tries to equalize. This flow generates tip vortices which in turn create downwash. And from the downwash effects we get induced drag.

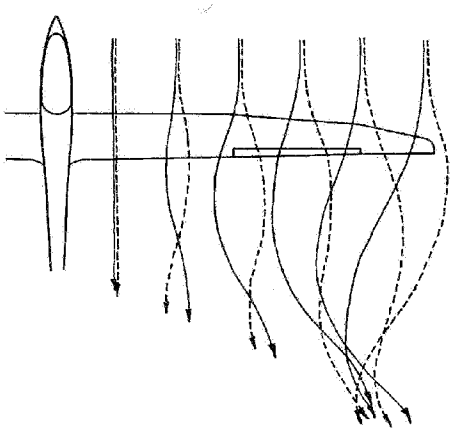

Fig. 2 Spanwise flow on a finite wing - solid lines, upper surface; dashed lines, lower surface.

Figure 3. Illustration of Spanwise flow

However it should not be inferred that the wing tip is the "gateway" for the flow. More accurately it helps define the nature of the pressure gradient, and in turn its pressure effects are felt across the wing. For most aircraft, the actual path for most of the flow that leads to vortex formation is across the leading edge of the wing, and not the tip. Figure 1 illustrates this property.

When a wing is swept back it will experience "leakage" around the leading edge. These create *leading edge vortices* which contribute to the overall induced drag, and are much less dependent on the geometry of the wingtip. In fact, for the swept wing with a sharp wing tip, the vortex formation is defined entirely by "leakage" as the path for the flow avoids the tip all together. Figure 2 shows how the leading edge vortices that contribute to downwash actually form inboard, and not at the wingtip.

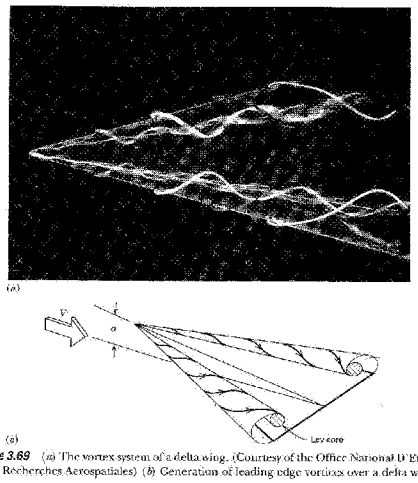

Figure 3.69 (*a*) The vortex system of a delta wing. (Courtesy of the Office National D'Etudes et de Recherches Aerospatiales) (*b*) Generation of leading edge vortices over a delta wing.

Figure 4. Leading Edge Vortices Over Swept Wing

Further, crescent wingtips also significantly displace the formation of tip vortices from the wingtips inward, as a consequence of the rapidly changing sweep.

Applied to Richard's Design: Richard's design shows that the main wing planform is a swept wing with crescent wing tips. It would certainly experience "leakage" about the main span, and high "leakage" about the crescent wing tips.

When it comes to evaluating the span efficiency **e** for Richard's design, the actual orientation of the endplates would have a much diminished effect because for this planform it is clear that the wingtip "leakage" does not fully define the flow path.

Section Conclusion (1):

- **(SC-1a)** Due to the flow "leakage" due to planform sweep and crescent wing tips, the path for a significant portion of the flow that contributes to vortex formation is independent of the wingtips.
- **(SC-1b)** Because of (a), the effective aspect ratio will be much less sensitive to endplate orientation.

SECTION 2

Adverse Yaw: It is important to emphasize that a major component of adverse yaw is in fact the induced drag differential created by asymmetric lift distributions, that points the aircraft in the opposite direction to the turn. This is currently the case for all aircraft that employ ailerons. The applicant will later show that in much the same manner as illustrated below, the asymmetric lift distributions seen in Richard's design in fact causes adverse yaw in much the same manner as seen in Figure 5.

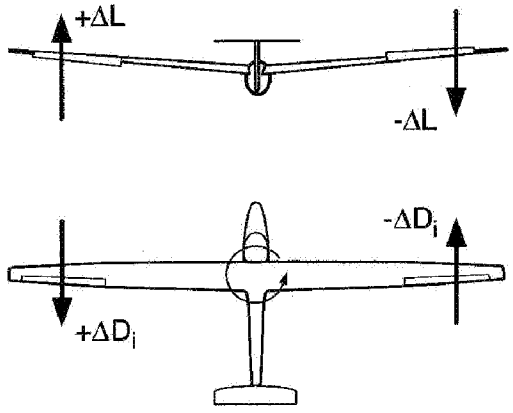

Fig. 73: Adverse yaw: the asymmetric lift distribution due to aileron deflection produces a spanwise variation in induced drag and, in turn, a yaw moment away from the direction of aileron input.

Figure 5. Induced Drag Contribution to Adverse Yaw

Section Conclusion (2):

- **(SC-2a)** If an aircraft, in order to execute a turn, creates an asymmetric lift distribution that results in an induced drag differential that points the plane in a direction opposite to the turn, this induced drag differential is one of the components of **Adverse Yaw.**
- **(SC-2b)** All fixed wing aircraft with ailerons exhibit the characteristic described in (2a) when turning.

SECTION 3

Endplates: *Basic Principle.* When adding endplates to the tip of a wing, keeping the span constant, the volume of air (stream tube) deflected by that wing when lifting, becomes increased. As a consequence, downwash and induced angle of attack are reduced. *With regard to lift*, it does not matter whether the plates are attached to the upper or lower side of the wing, or symmetrically extending up. When adding a pair of endplates to a wing, the effective span efficiency **e** is increased.[1]

"The effect is rather indifferent as to the particular location and position of the plates. Within reasonable limits, it thus seems to be unimportant, whether the plates are moved up or down in relation to the plane of the wing, or placed nearer to the leading or trailing edge of the foil section."[2]

Known Solution: Span efficiency **e** for wings with endplates is a function of the ratio of the height of the endplate to wingspan.

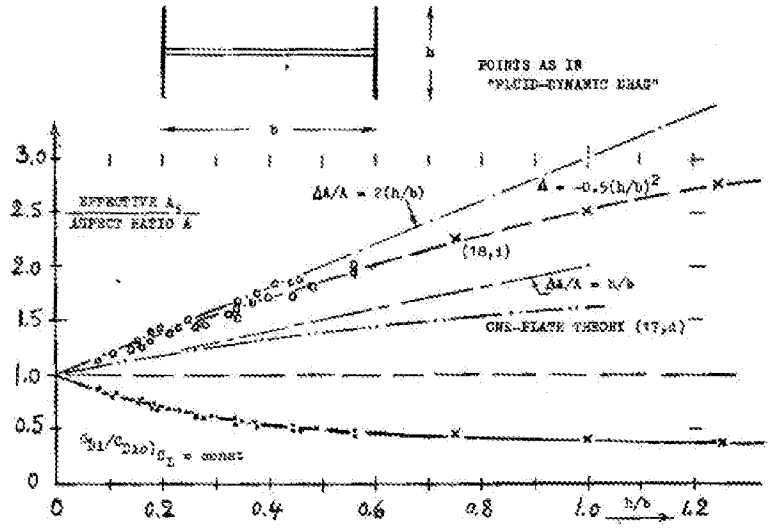

Figure 6. Effective Aspect Ratio vs. h/b (Span Ratio/Endplate Height) Ref. [2]

Applied to Richard's Design: The endplate's primary function is to restrict flow, and it is in this manner that it influences induced drag. It is a pressure gradient barrier. As stated above, the small changes in orientation have negligible effects. However, as will be discussed in later sections, larger changes in orientation affect the span efficiency **e**, and although changes at small endplate hinge angles are small, a predictable trend does exist.

Section Conclusion (3):

- **(SC-3a)** Known solutions for effective aspect ratio for a wing with endplates exist, based on wind tunnel data. Relationship is known to be a function of wingspan and endplate height.
- **(SC-3b)** Repositioning of endplates has no effect on **lift** of the main wing section.

SECTION 4

Winglets: Winglets differ from endplates in that winglets do not strive to reduce induced drag so much as it creates its own induced flow field that is adverse to the formation of downwash. Pioneered in the 1970's, it was found that for induced drag reduction the vertical surface at the wingtip must efficiently produce significant side forces. These side forces are required to reduce the lift-induced inflow above the wing tip, or the outflow below the tip.[6]

"A winglet, unlike a simple fence that merely restricts the spanwise flow around the tip, uses an aerodynamic load to produce an (induced) flow that interacts with that of the main wing to reduce the amount of spanwise flow and, therefore, the induced drag"[8]

The induced flow of the winglet is created in the exact manner that the main wing produces downwash, hence the term "winglet".

Winglets applied to Richard's design: Winglets exhibit characteristics that influence span efficiency (in the same manner as endplates) and wing lift coefficient, whereas classic true vertical endplates only influence span efficiency. It is clear that when Richard's endplates are deflected, they behave in a manner that exhibits the properties of winglets.

Section Conclusion (4):

- **(SC-4a)** Richard's endplates exhibit qualities that influence span efficiency **e,** and spanwise flow, but in a different manner than traditional endplates and traditional winglets.

SECTION 5
Analysis of Endplate Effects on C_L and Ae

Plate Orientation Contribution to Total Lift C_L and Induced Flow

Wing Total Lift C_L: Total lift of the wing is simply the summation of the lift produced by the main span with the vertical component of lift produced by the endplate at a given hinge deflection. Main span lift is solved for by classical aerodynamic methods (endplates have no effect on lift of main span, see **SC-3b**). Orientations of endplates solved for by creating endplate-fixed coordinate system and solving for their Euler angles relative to the aircraft body-fixed system as a function of deflection angle hinge angle. Relative winds are computed in the same manner. Normal force on endplate computed, and the component of which is in the lifting direction is the endplate contribution to total lift. Total wing lift coefficient, C_L, as a function of endplate hinge angle is computed from these components. This represents the same textbook solution to wing total lift found in any undergraduate aerodynamic text.[14]

Section Conclusion (5):

- **(SC-5a)** Textbook solution to wing total lift C_L, as a function of endplate hinge deflection.

SECTION 6
Plate Orientation Contribution to Effective Aspect Ratio Ae

Effective aspect ratio is the product of wing aspect ratio **A**, and wing span efficiency **e.**

Wing Aspect Ratio A: Textbook calculation of wing aspect ratio based geometry.

Wing Span Efficiency e: Wing span efficiency **e** is the dominant factor in determining effective aspect ratio **Ae**. We will begin by itemizing the contributioins of Richard's endplate orientation, and their effects on span efficiency.

Endplate orientation effects on span efficiency, **e**:

- **Endplate Shape** – Shape of endplate has been shown to be unimportant. Riebe and Watson found that span efficiency is "…relatively independent of end-plate shape. This is as would be expected, as the theory indicates that regardless of wing aspect ratio, the increase in A'/A <span efficiency, **e**> is dependent on end-plate-height to wing-span ratio".[5]
- **Endplate Sweep** – Richard's endplates experience a small rotation, changing their sweep as they are deflected. This effect is truly inconsequential in comparison to the major changes in dihedral angle. Even so, the effect of sweep variations has been found to be a negligible influence on total wing performance.[8]
- **Endplate Toe (Angle Incidence)** – "When toeing in or out a pair of end plates, symmetrically attached to the lateral edges of a wing, "nothing" changes aerodynamically."[1] This is the extent of incidence on span efficiency **e**, which is nothing. However, toe does create increases/decreases to lift when the endplate is rotated about an angle and their contribution is to wing total lift $\mathbf{C_L}$ is shown in **(SC-5a).** However, wind tunnel results indicate that span efficiency **e**, is not influenced by endplate toe.
- **Endplate Twist** – these are flat endplates, there is no twist.
- **Endplate Height** – The total height of the endplates as well as their relative height shift above and below the wing plane does affect span efficiency. This is included in the model of span efficiency as outlined in the next section.
- **Endplate Dihedral** - Span efficiency is sensitive to dihedral angle. This is included in the model of span efficiency as outlined in the next section.

Thus the span efficiency is dependant on height of endplate above and below the wing, as well as the dihedral angle it makes due hinge angle deflection above and below the wing.

Section Conclusion (6):

- **(SC-6a)** Wing span efficiency **e** is a function of endplate height above and below the plane of the wing, as well as the dihedral angle (hinge deflection angle) of the plate.

SECTION 7

Calculation of Span Efficiency e for Richard's Design: Established solutions exist for estimating the induced drag span efficiency factor **e**, for non-planar lateral wing forms based on basic wing configurations which have exact solutions based on known span efficiencies for non-planar wing configurations (Ref. [10], Ref. [9]). Using these methods and exact solution for span efficiency was calculated for **e** as a function of endplate deflection that incorporated all relevant deflection variables listed in **(SC-6a)**. The solution was then validated against the known solution for endplate span effectiveness based on wind tunnel data **(Figure 6.)**, as well as span efficiency trends due to dihedral reported in the aerodynamic literature.

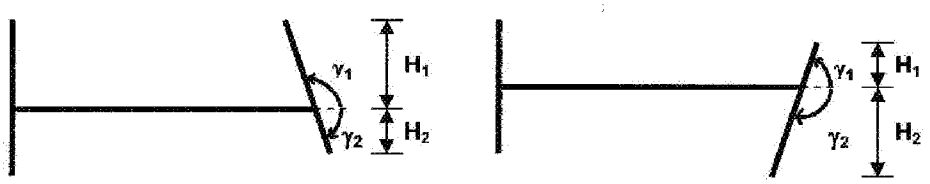

Figure 7. Illustration of Span Efficiency Solution

Section Conclusion (7):

- **(SC-7a)** Exact solutions for span efficiency **e** of arbitrary non-planar wing forms such as seen in Richard's design already exist[9] and have been validated against known span efficiency solutions based on wind tunnel data. It is by this means that span efficiency **e** and effective aspect ratio **Ae** were calculated as of function of endplate hinge deflection angle.

SECTION 8
Explanation of Trends Wing Span Efficiency Solution

Span efficiency **e** and by extension effective aspect ratio **Ae** follow certain trends that merit a qualitative explanation.

Endplate Height Above vs. Below Wing: To illustrate the effects of endplate height on span efficiency:

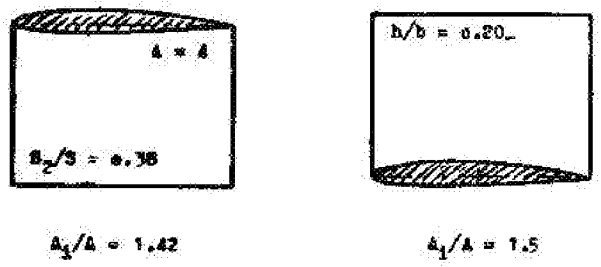

Figure 8. Endplate Influence on Span Efficiency Above/Below Wing, Ref [2]

The reader should note that the span efficiency **e** (denoted Ai/A in this reference) which is calculated from wind tunnel results, is listed as 1.42 for the plate when oriented below the wing, and 1.5 when oriented above (5.6% difference). What this shows is that when an endplate is oriented above a wing, it has a greater ability to reduce induced drag than when oriented below.

The same property holds true for winglets. In terms of span efficiency **e** classic analytic theory does not discriminate between positive and negative dihedral. However, Eppler describes in Reference [11] that the *actual* difference in induced drag between positive and negative winglets can be as much as 11%, with the advantage going to positve dihedral. This is why the overwhelming majority of winglets seen on aircraft today bend up above the wing plane.

Section Conclusion (8):

- **(SC-8a)** Plate surface mounted above wing is more effective at reducing induced drag than when mounted below, when comparing positive to negative dihedral angle for all deflections
- **(SC-8b)**When a plate has portions both above and below the wing in equal measure, the upper portion contributes more to reducing induced drag than the lower, and is thus the dominant half of the plate

SECTION 9

Endplate Dihedral (Cant) Inward vs. Outward: To illustrate this property, the following winglet diagram:

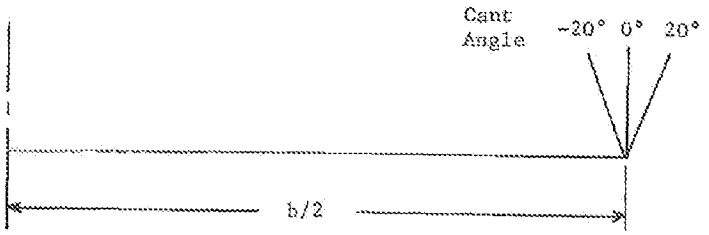

Figure 9. Representation of Dihedral Angle

Outward Dihedral (Cant): C. P. van Dam [12] performed parametric wind tunnel studies on the effects of winglet orientation on the span efficiency **e**, as part of a larger investigation on winglets. For the configuration shown, test results[12] demonstrated that "Induced drag will decrease with increasing cant(dihedral)", that is, as the plate swings from full outward orientation towards the vertical (rotating from an angle of +90° to 0° in above figure), span efficiency continuously increases. This is the identical result confirmed by independently by Hoffstadt [8], and Heyson and Riebe [6] based on their own independent experimental results.

Inward Dihedral (Cant): As the rotation of the dihedral (cant) angle passes through the vertical and the plate points inward (rotation from 0° to -20°), the ***span efficiency continues to increase*** beyond the efficiency seed when oriented vertically. Reference [12] goes on to state "however, it is possible to realize ***gains in induced efficiency*** at a very small penalty in root bending moment ***if the winglet is canted inward***". This result is also confirmed by the results of Reference [6] which states, "<wind tunnel results> show if the winglet is canted(dihedral) inward, it is possible to realize significant gains in induced efficiency…"

Further, ***the behavior is similar regardless if the plate is oriented upward or downward***, span efficiency **e** increases as in. Again, in terms of span efficiency **e** classic analytic theory does not discriminate between positive and negative dihedral. Thus, when a downward oriented winglet is canted inward, span efficiency also continuously increases is higher as it is rotated from outward to inward. However, when comparing actual magnitudes of induced drag, an upward oriented endplates will always show a higher span efficiency for a given deflection than its negatively deflected counterpart **(see (SC-8a)).** Combining the two results of efficiency trends for dihedral angle with the known dominant span efficiency effects of upper plate over the lower, reveal that the ***span efficiency trend for Richard's design follow the span efficiency trend of the dominant upper portion of the endplate when it comes to evaluating the efficiency changes of the plate due to hinge deflection.*** This is in fact the computed result when applying the span efficiency solutions of Ref. [9].

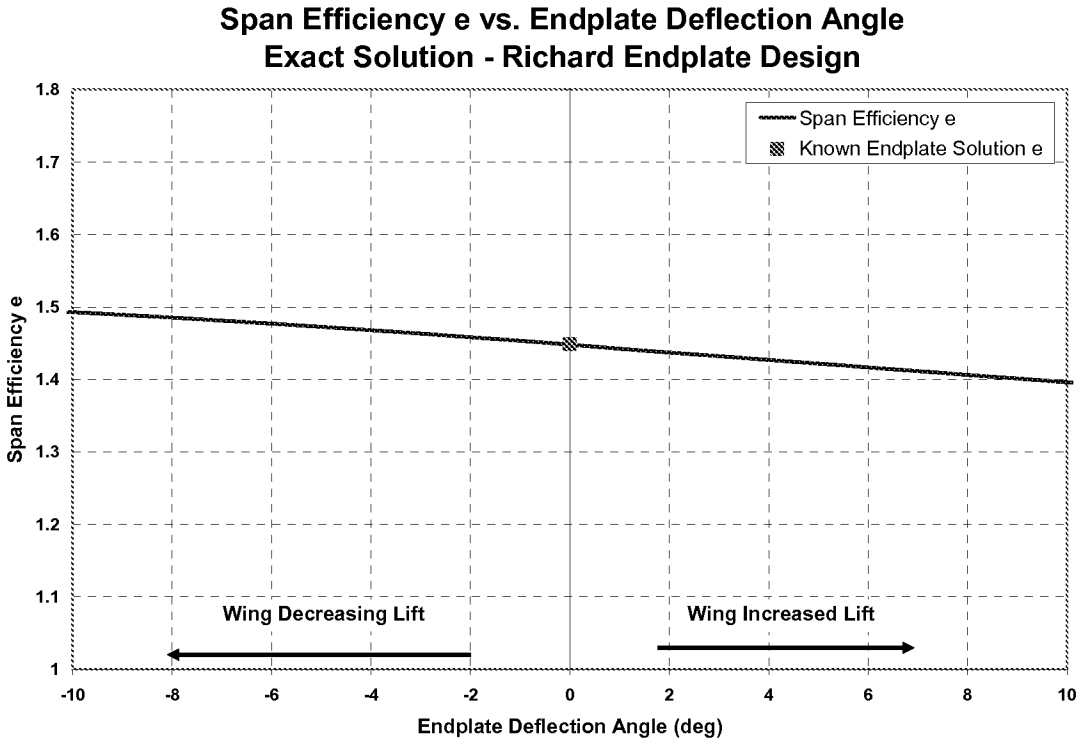

Figure 10. Span Efficiency e vs. Endplate Deflection – Small Angles

Applied to Richard's Design: The effect on span efficiency **e**, is the summation of the span efficiency characteristics just listed. For an endplate:

- plate structure above the wing has a greater ability to reduce induced drag than that oriented below the wing when at the same dihedral angle
- span efficiency increases continuously as cant rotates from outward to inward[9]
- height shift of endplate above and below the surface of the wing as a function of hinge deflection angle **(see SC-8a)**

Combining these properties predicts that the behavior of span efficiency as a function of endplate deflection angle is determined by the **orientation of the upper plate.** That is, when the upper plate is rotated inward span efficiency is greater than when it is at the neutral position, and at the neutral position is efficiency is greater than it is when the upper plate is rotated outward.

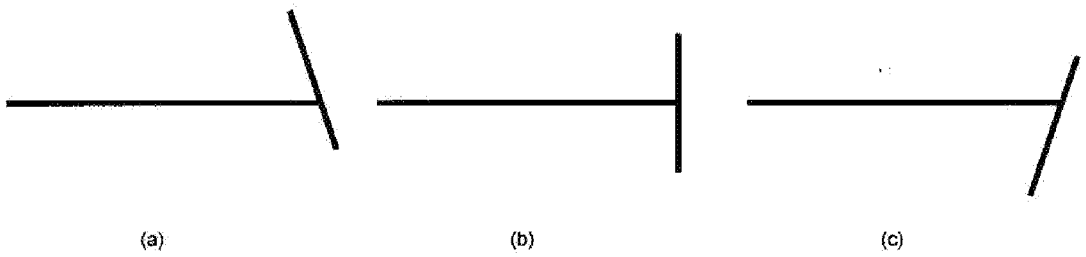

Figure 11. Span efficiency comparison: $e_a > e_b > e_c$

Shown above is this effect, where $e_a > e_b > e_c$. An exact solution for span efficiencies for arbitrary lateral-vertical planforms based on known exact solutions has been formulated by Reference [9]. When applied to Richard's endplate configuration it confirms this trend.

Section Conclusion (9)

- **(SC-9a)** Endplate span efficiency **e** increases continuously as the upper half of the plate swings outward to inward up to inward for small angles
- **(SC-9b)** The result indicates that when an endplate is deflected into the increased lift position that it is less effective at reducing induced drag than when it is deflected into the decreased lift position. This indicates that for deflections in the range about the neutral position span efficiency **e**, and by extension effective aspect ratio **Ae**, favors the production of adverse yaw
- **(SC-9c)** All trends shown are consistent with known test results of planform with similar configurations for Richard's endplate design.

SECTION 10
Numeric Analysis of Richard Endplate Design

The applicant performed an aerodynamic analysis of Richard's design, considering only the variables which contribute to induced drag, namely solving for wing total lift $\mathbf{C_L}$, and effective aspect ratio **Ae**.

$$\mathbf{C_{Di} = C_L^2/(\pi * Ae)}$$

Model Details

Details of the aerodynamic modeling are as follows:

- All calculations were done on single wing half which rotated its endplate through the range of deflections possible in Richard's design.
- Specifications of aircraft solved for from measured geometry shown in Richard's drawings, non-dimensionalized to coefficient form, and listed in Appendix.
- Endplate planform modeled as ellipse, as shown in Richard's drawings.
- Orientations of endplates solved for by creating endplate-fixed coordinate system and solving for their Euler angles relative to the aircraft body-fixed system as a function of hinge angle. Details listed in Appendix.
- NACA 2412 airfoil selected for wing (same as Cessna 172 Skyhawk)

Endplate Contribution to lift: Standard textbook solution for ellipse planform at a given orientation to the freestream.

- Calculated aerodynamic forces for endplate geometry, ellipse assumed.
- NACA 0012 airfoil selected for endplate (neutral airfoil, approximated dimensions seen in Fig. 1 of Richard's patent).
- Neutral airfoil – produced zero side forces when hinge angle = 0
- Relative wind vectors to endplate as a function of hinge deflection solved from Euler angles
- Computed relative wind and lift as a function of hinge deflection angle.

Endplate Contribution to Effective Aspect Ratio: The wing effective aspect ratio (**Ae)** is the product of the wing aspect ratio **A,** and the span efficiency **e**.

- **Wing Aspect Ratio A:** Textbook calculation of wing aspect ratio based geometry.
- **Wing Span Efficiency e**: Established solutions exist for estimating the induced drag span efficiency factor **e**, for non-planar lateral wing forms based on basic wing configurations which have exact solutions based on known span efficiencies for non-planar wing configurations (Ref. [10], Ref. [9]). Using these methods and exact solution for span efficiency was calculated for **e** as a function of endplate

deflection angle. Details discussed in **(SC-7a)**. Results validated against known solutions for span efficiency **e**, as applied to Richard's design.

Aerodynamic Analysis Results and Discussion
Richard Endplate Design

The below figure represents the calculated results of induced drag felt by one wing of Richard et al Endplate Design as a function of hinge plate deflection.

Wing Induced Drag – Full Endplate Deflection Range

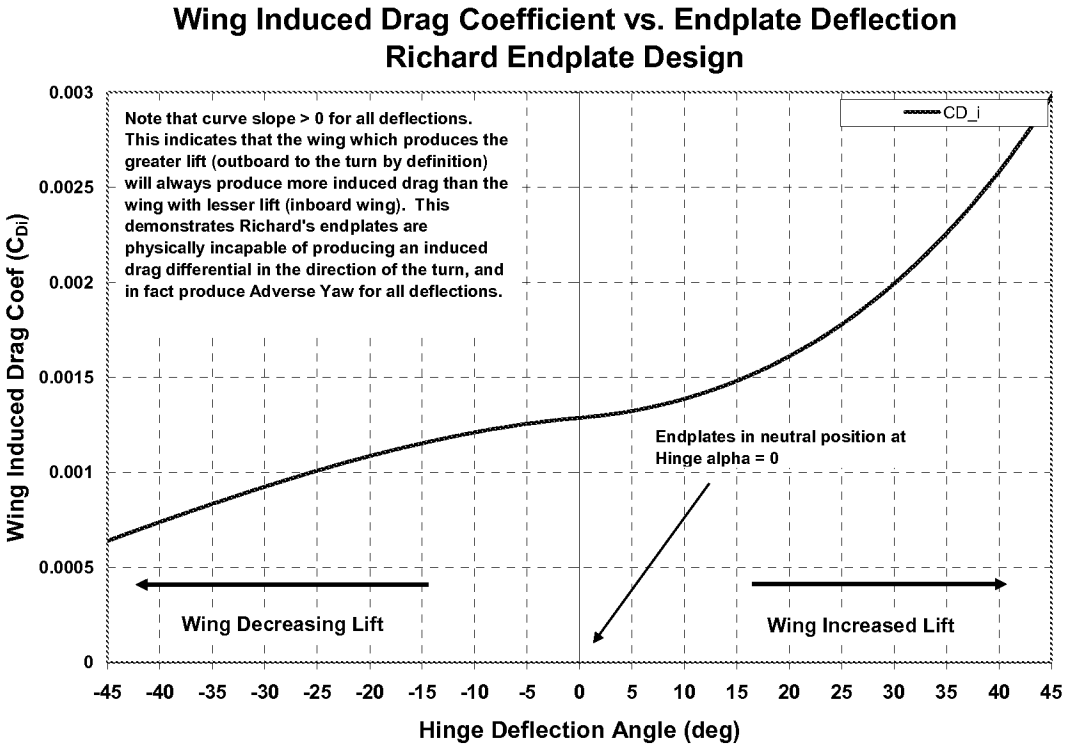

Figure 12. Wing Induced Drag Coefficient vs. Endplate Deflection Angle

Positive endplate hinge deflection angle indicate the plate has been rotated downward into the increased lift position, as shown on the right side of **Fig.2** from Richard's patent, and negative hinge deflection angles represent a plate rotation upward to the decreased lift position, as shown in the left side of **Fig.2** from Richard's patent. A hinge deflection angle of 0 represents the endplate in the neutral position, as shown on the right side of **Fig. 3** of Richard's patent.

The results show that induced drag increases continually with increasing wing total lift as a function of hinge deflection angle, with no inflections. What this means is that for all hinge deflection combinations shown in Richard's design that produce an asymmetric lift distribution that cause the aircraft to roll into a turn, **the wing which**

produces the greater lift will always produced a higher amount of induced drag. The wing which produces the greater lift is by definition the wing outboard to the turn. And if the outboard wing to the turn produces a greater induced drag, then it is considered **adverse yaw.**

Therefore, after careful analysis of the Richard et al's endplate design it is clear that **for all deflection combinations the design presented by Richard et al in his patent will produce an induced drag differential in the form of adverse yaw.**

Wing Induced Drag – Small Hinge Deflections

Presented here are the same results for endplate deflections at small angles. The result is the same as presented above, that is induced drag increases continually for increased wing lift.

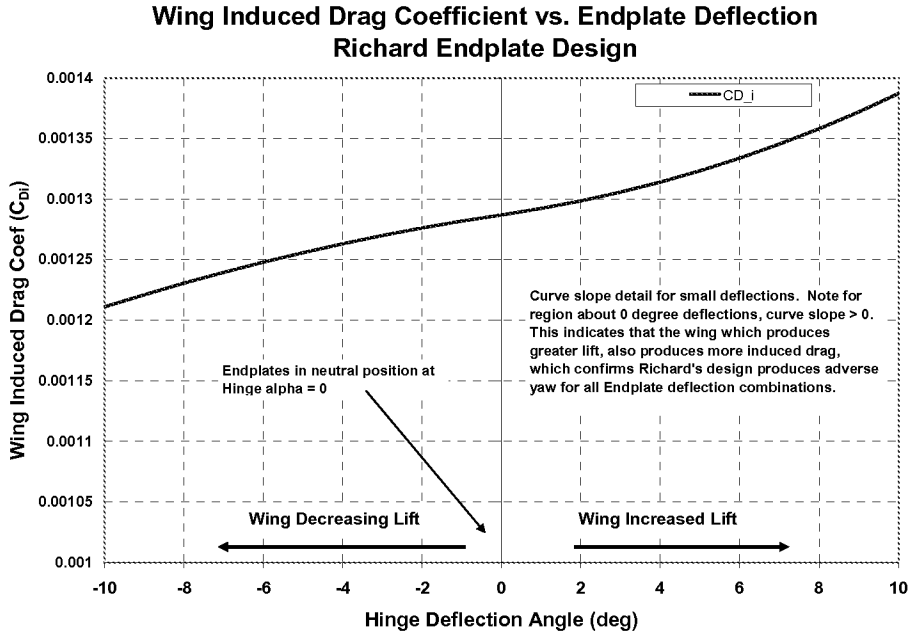

Figure 13. Wing Induced Drag Coefficient vs. Endplate Deflection (Small Angles)

However, it has been noted by the examiner that at small hinge deflection angles about zero, changes in wing total lift coefficient C_L are very small. This is true, however at small angles effective aspect ratio **Ae** behaves in a manner which produces adverse yaw to the turn.

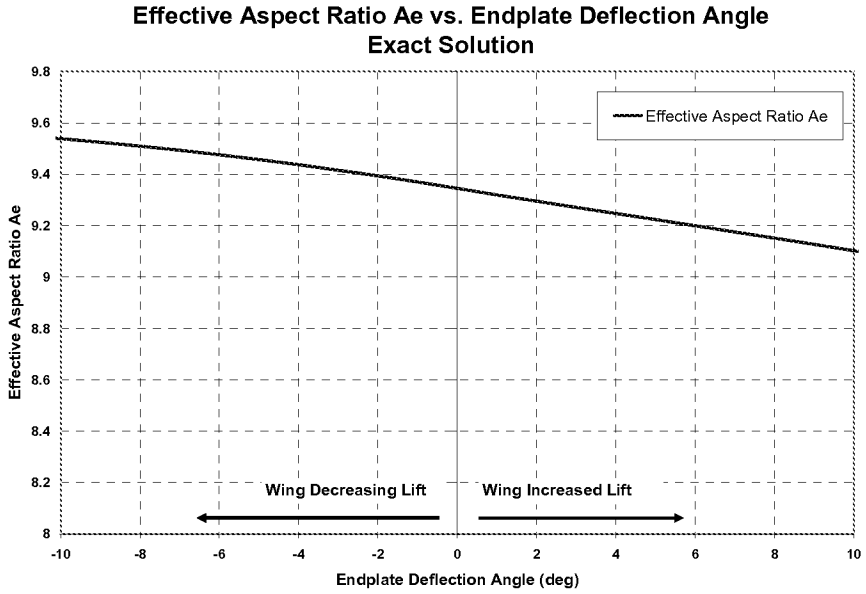

Figure 14. Effective Aspect Ratio Ae vs. Endplate Deflection (Small Angles)

The graph of the effective aspect ratio **Ae** shows that at endplate deflections for small angles the effective aspect ratio behaves in a manner that will promote the trend of adverse yaw seen in the previous 2 charts. That is, as wing lift increases, effective aspect ratio **Ae decreases continuously**. This means that the more lift a wing produces, the less efficient it will be, the more induced drag it will produce. This will **always result in adverse yaw produced for small endplate deflections, regardless of their combination.** This is same result concluded in **(see SC-9b).**

It should also be noted that effective aspect ratio **Ae,** only drives adverse yaw trends ***at small hinge angles.*** Once again, the equation:

$$C_{Di} = C_L^2/(\pi * Ae)$$

From inspection of the equation it is easy to see that induced drag is the function of the square of wing lift coefficient C_L. So it follows that increases or decreases in C_L have an exponential effect on induced drag, making it the dominant component driving in net induced drag effects. In this manner Richards design will demonstrate adverse yaw in the same manner as all other aircraft with ailerons, the wing with the greatest lift produces the most induced drag and thus adverse yaw to the turn. This is the same result shown in **(see SC-2a).**

Thus for Richard's design, we can conclude for all combinations of endplate deflections, adverse yaw is produced. This is primarily dominated by effects of wing total lift CL, and its tendency to create adverse yaw **(see SC-2a).** But at small endplate deflection angles it is the unfavorable behavior of the effective aspect ratio **Ae**, which can only be seen because of the significant decrease in C_L effects. Richard's endplate flight control design has been shown to produce adverse yaw for all combinations of endplate

deflections, and does not employ "The Method of Induced Yaw" as a means of flight control.

Section Conclusion (10)

- **(SC-10a)** Richard's endplate design has been shown through a numerical aerodynamic analysis to produce adverse yaw for all combinations of endplate deflections. All effects contributing to induced drag as a function of endplate hinge deflection angle were solved for, and nowhere does it produce an induced drag differential in the direction of the turn.
- **(SC-10b)** The adverse yaw produced is dominated by the asymmetric wing lift coefficient effects $\mathbf{C_L}$ for the majority of the deflection angles in the same manner that occurs with most aircraft with ailerons **(see SC-2a).**
- **(SC-10c)** At small endplate deflection angles, the induced drag effects are dominated by the trends in effective aspect ratio **Ae, as** $\mathbf{C_L^2}$ effects are diminished. The direction of the trend at in **Ae** at small angles effects yaw to the turn in an unfavorable manner, and thus the endplates create adverse yaw at small deflection angles. The trend agrees with the conclusion discussed in **SC-10a** and **SC-9b.**

Analysis Summary

Richard's design can only produce an induced drag differential that creates additional adverse yaw, rather than overcoming it.

The formation of induced drag for a wing is the function of the square of the wing lift coefficient to the effective aspect ratio.

$$C_{Di} = C_L^2/(\pi * Ae)$$

Through a thorough analysis, the applicant has examined the aerodynamic properties of the Richard's endplates and solved for the individual effects on C_L^2 and **Ae** as a function of endplate deflection. What was discovered was that with regard to induced drag formation, the wing which produces the greater lift (outboard by definition), will always produce greater induced drag, for all combinations of endplate deflections. This result insures that for Richard's design the net induced drag differential created by coupling of the asymmetric lift distribution (contained in C_L^2) and the asymmetric geometric effects of endplate deflection (contained in **Ae**), will create a net induced drag differential that **always creates adverse yaw**, pointing the aircraft in a direction opposite to the turn for all conditions. As stated in Claim 1 of Mr. Fairchild's patent application:

> 1. (currently amended) A method of controlling an aircraft in a turn without the use of ~~a~~ rudder control by producing induced yaw, comprising: creating a net induced drag differential between an inboard wing to the turn and an outboard wing to the turn, the net induced drag differential being created in such a manner that the net induced differential overcomes adverse yaw produced by the outboard wing.

Richard's design can only produce an induced drag differential that creates additional adverse yaw, rather than overcoming it. No where does Richard et al.'s endplate design employ the method of flight control expressed in Claim 1. of the current application under review.

Correlation of Examiner's Statements to Current Analysis

1. *"With respect to Applicant's arguments and comments pertaining to the rejection of claims 1, 2, 4, 6 and 8, Examiner respectfully assert that Applicant has misinterpreted the basis of the outstanding rejections. During the telephonic interview on 1/26/2007, the "attendees" (Applicant, Examiner and Senior Examiner) discussed the rejections and the use and perceived definition of "induced drag" and "induced yaw". However, there was no agreement reached in relation to term usage, the applied reference, or the current or future status of this application or any corresponding office action. As stated in interview, Examiner fully understands the art specific difference between "induced drag" and inducing drag. Applicant has asserted that Examiner has misinterpreted the meaning of "Induced Drag" and therefore improperly applied the Richard et al. reference. However, Examiner respectfully maintains, as stated in interview and non-final rejection, that the end plates disclosed by Richard et al are capable of, to at least some degree, influencing the movement of wingtip vortices from the bottom of the wing to the top (component of "Induced Drag") thus creating a "net induced drag differential". Examiner has never indicated that the term "Induced Drag" has been interpreted as related to parasite drag or applied in the context of a verb. In keeping with the assigned definition of the term "induced yaw" from Applicant's specification,* ***Examiner respectfully maintain that the inboard wing "to the turn" disclosed by Richard et al "experiences" a higher Induced Drag, to at least some degree, than the outboard wing "to the turn", because it is Examiner's opinion that the when the end plate of Richard et al is angled out as shown in Richard et al fig. 3,*** *the higher pressure under the wing will have an easier path around the end plate/wingtip and thus induce a higher degree of downwash (resulting in at least some increase in Induced Drag). Further, Examiner maintains that* ***the Richard et al patent merely need to be capable of overcoming the lowest potential level of adverse yaw (smallest amount of aileron deflection). Examiner believes that it is reasonable to assume that the adverse yaw created by the smallest possible aileron deflection can be overcome by manipulating the Richard et al device as shown in fig. 3 as described in Richard et al***

Comment Analysis:

Aerodynamic Analysis Results

Let us begin by stating that for unusual configuration changes seen in Richard deflecting endplate design, the individual components of the induced drag equation,

$$C_{Di} = C_L^2/(\pi * Ae)$$

all have established exact solutions that come from aerodynamic literature. Wing total lift C_L is the combination of lift force on the main wing with vertical lift force on the endplate as a function of endplate rotation, and represents the standard solution found in any aerodynamic text **(SC-5a).** Wing aspect ratio **A** represents a simple geometric calculation. And most notably, the exact solution to span efficiency **e** for arbitrary-lateral wing configurations (including endplates at arbitrary orientation and height, **see Figure 7.**), as seen in Richard's design, exists and can be solved for as a function of endplate deflection **Ref. [9].** Using these components the applicant was able to solve for the actual induced drag produced by the wing half as a function of endplate deflection.

The analysis focused only on the production of induced drag as a function of endplate deflection, to establish which ***direction*** the net induced drag differential would yaw the plane, which if unfavorable is by definition is *"adverse yaw"*. The results of this

analysis **(Figures 12-14 and SC-10a,b,c)** are displayed in the "**Aerodynamic Analysis Results and Discussion**" section, indicate that for all possible combinations of endplate deflections seen in Richard's design that can cause an aircraft to turn, ***the wing that produces the most lift (outboard to the turn by definition) will always produce a larger amount of induced drag and thus will create a yawing moment unfavorable to the turn known as "adverse yaw".*** To quote claim 1:

For Induced Yaw to exist as a method of control, the wing which produces more lift must also generate less induced drag than the opposite wing.

Per results of the aerodynamic analysis, Richard's endplate design is only capable of producing adverse yaw to the turn, and does not utilize "The Method of Induced Yaw" as defined by claim 1.

Examiner's Comments

Here the applicant will present a point by point qualitative and mathematical explanation for the aerodynamic forces at play, to aid with understanding the results and how they specifically apply to Examiner's comments concerning Richard's endplate method of flight control, as shown in **Fig. 3**, of Richard patent.

Examiner states:

"Examiner respectfully maintain that the inboard wing "to the turn" disclosed by Richard et al "experiences" a higher Induced Drag, to at least some degree, than the outboard wing "to the turn", because it is Examiner's opinion that the when the end plate of Richard et al is angled out as shown in Richard et al fig. 3.

The left side of Fig. 3 represents the turn configuration where the left endplate is rotated above the wing in the "decreased lift" position, and the right endplate is in the "neutral" position. In this configuration the right "neutral" endplate will have greater lift than the opposite wing and will be the wing outboard to the turn for all deflection angles as shown in Fig. 3 for the "increased lift" position.

At Larger Angles.

(P1) Adverse Yaw has many components, and an unfavorable induced drag differentials pointing the aircraft in a direction opposite to the turn has always been considered one of them (Please refer to **Figure 5.** for confirmation). Aircraft with asymmetric lift distributions, as Richard's design as shown in Fig. 3 has an asymmetric lift distribution, the "neutral" plate being that with greater lift, will in turn produce greater induced drag, and yaw the aircraft in an unfavorable direction. This is the generalized result, but what it shows is that the induced drag differential that leads to adverse yaw is a function of increased lift, $\mathbf{C_L}$. From inspection of the induced drag equation, we see that induced

drag grows exponentially with $\mathbf{C_L}$. This means that wing lift is the dominant effect that establishes the induced drag trend for Richard's endplates as a function of deflection most angles (not small angles). What this implies is that as the total wing lift grows large, so does induced drag. Thus the wing that produces the most lift (outboard to the turn, by definition) will produce the greater induced drag, the effect of which will be adverse yaw. This exactly demonstrated the predicted solution as shown in **Figures 12 and 13**. This means that for Richard's endplate design, as depicted in **Fig. 3**, because the wing with the endplate in the neutral position produces the greater total lift, it would follow that it would produce greater induced drag than the opposing wing with "decreased lift" for deflections, excluding small angles, due to the exponential contribution that wing lift, $\mathbf{C_L}$. This of course would create adverse yaw to the turn. This is also the same result shown in **Figures 12 and 13.**

Excerpt 2 of 2:

> *"... the Richard et al patent merely need to be capable of overcoming the lowest potential level of adverse yaw (smallest amount of aileron deflection). Examiner believes that it is reasonable to assume that the adverse yaw created by the smallest possible aileron deflection can be overcome by manipulating the Richard et al device as shown in fig. 3 as described in Richard et al"*

At small angles:

(P2) Endplates positioned above wing more effective at reducing induced drag than endplates positioned below wing, when comparing both positive and negative area balance; and also when comparing positive and negative dihedral angles. Please refer to **"Endplate Height Above vs. Below Wing"** Section, **Figure 8, (SC-8a), and (SC-8b).** To summarize, when an aircraft has an endplate is mounted above the wing it experiences a higher wing span efficiency **e** than when it is mounted below (illustrated in **Figure 8,** source: **Ref [2]).** The difference illustrated in span efficiency **e** in **Figure 8** calculated to be 5.6% in favor of the plate mounted above the wing.

The same span efficiency **e** property holds true for winglets, which capitalize on the same span efficiency properties as endplates. **Reference [11]** describes that the difference in induced drag between positive dihedral (above the wing) and negative dihedral (below the wing) winglets can be as much as 11%, with the advantage going to the positive dihedral. This fact is why the overwhelming majority of winglets seen on aircraft today bend up above the wing plane.

As applied to Richard's design.

When examining **Fig. 3** of Richard's patent, it is **clear** that the balance of area of the endplate is above the plane of the wing, where the left endplate is in the "decreased lift" position. When examining the right side of **Fig. 2** of Richard's patent, it is **clear** that the balance of area of the endplate is below the plane of the wing, where the right endplate representing the "decreased lift" position. And it is also clear that when these endplates are deflected and hinge angles that are equal in magnitude but negative to one another, they will each respectively exhibit the identical area shifts above and below the wing.

From the results mentioned above concerning induced drag differences for plates mounted above and below the wing: if we were to compare to the induced drag produced by an endplate at the opposite dihedral, that is at the same inward inclination but in the "increased lift" position (right side of **Fig. 2** of Richard's patent), we would know that the "decreased lift" position would produce less induced drag than the "increased lift" position. The difference in plate area above vs. below the wing is the reason for this, as is shown by **Ref [1]** and **Ref [11],** as discussed above.

This trend would continue as we continually decrease the magnitude of the angles smaller and smaller, while still maintaining equal balance between positive and negative dihedral. And always, the endplate mounted above the wing in the "lesser lift" position, would always produce less induced drag than the endplate mounted in the "increased lift" position.

As we approach the "neutral" position in our comparison (small angles), we establish the trend for induced drag at small angles. Namely that the induced drag produced by the endplate deflected at the "smallest amount of deflection" upward to the "decreased lift" position, will produce less induced drag than the "smallest amount of deflection" downward, due to the results shown at the beginning of **(P1)** concerning endplate area above and below the wing. It follows that the quantity of induced drag produced by the "neutral" position will reside between that of the upward "decreased lift" position and the downward "increased lift" position.

(P2) CONCLUSION: As applied to Richard's design at small deflection angles the trend for induced drag is as follows: **At small angles: the induced drag produced by the wing when the endplate is in the "increased lift"(Fig 2., right side) position is greater than the induced drag produced while the endplate is in the "neutral position" which is still greater than the induced drag produced by wing in the "decreased lift".** Specifically, for **Fig. 3** of Richard's design, this shows that the wing with the endplate in the "neutral" position will create more induced drag than the wing with the endplate in the "decreased lift" position, thus creating adverse yaw to the turn. This is the result shown in **Figure 13**. Note that induced drag increases continuously with wing total lift for small angles.

(P3) Further, it follows as an extension of the first 2 paragraphs of **P2** that when a plate has portions both above and below the wing in equal measure; the upper portion contributes more to reducing induced drag than the lower, and is thus the dominant half of the plate. **(SC-8b)**

In terms of dihedral, a single plate or winglet when mounted above the wing (see **Figure 9**), it exhibits a continuous increase in span efficiency **e,** as the plate rotates from an outward dihedral inward. (**see Endplate Dihedral (Cant) Inward vs. Outward Section**), **Ref [12], Ref [6].** Combining the facts of upper plate dominance in reducing induced drag, and span efficiency increase due to inward cant over both outward and neutral, it follows that when the dominant upper plate rotates inward, it will experience an increase in span efficiency **e**, and a reduction in induced drag.

As applied to Richard's design in **Fig. 3** at small angles, when the dominant upper half of the plate rotates inward, as it does in the "decreased lift" endplate configuration, then follows that the wing will experience an induced drag decrease over the induced

drag felt for the wing with the endplate in the "neutral" position. This would in turn create adverse yaw to the turn for small angles. This is the result also shown in **Figure 13.**

Mathematically:

In picking small angles for study of the configuration in **Figure 3**, the examiner has identified the exact place that wing lift coefficient, $\mathbf{C_L}$, has lost its dominance in the induced drag equation. This is of course where deflection angles approach zero (the endplate "neutral" position), that the change in wing lift as a function of endplate hinge deflection angle goes to zero. Meaning, lift curve has no slope and wing lift is essentially constant. In the same manner, at small angles approaching zero, change in aspect ratio, **A**, goes to zero and aspect ratio is constant. Therefore the change in the induced drag coefficient at angles close to zero is only dependent only on span efficiency, **e**, as **A** and $\mathbf{C_L}$ can be considered constant.

The exact formulation for span efficiency, **e**, of arbitrary, non-planar wing forms such as seen in Richard's design as a function of endplate deflection are given by **Reference [9],** and is plotted in **Figure 10**. The curve plotted shows that the change in **e** as a function of hinge plate deflection is ***not constant, but is continuously decreasing.*** Mathematically, this shows that at the hinge deflection of zero "neutral endplate position", the induced drag produced is continuously increasing with increasing lift, that is as the endplate rotates from the "decreased lift" to "neutral" to "increased lift" configuration. This mathematically validates the conclusion of **(P2)**, and demonstrates for the configuration as shown in **Fig. 3** of Richard's patent; that the wing with the endplate in the "neutral" position will produce more induced drag than the wing in the "decreased lift" position, thus creating adverse yaw.

Additionally, it is important to note that plotted on the graph of **Figure 10,** is the exact span efficiency solution for wings with vertical endplates based on the wind tunnel data displayed in **Figure 6** for Richard's aircraft configuration. This data is taken from **Ref [1],** and represents span efficiency results for wings with endplates for a variety of plate height/span ratios. This constitutes independent validation of the span efficiency **e** predictions provided by the method given in **Ref. [9].**

Correlation of Examiner's Rejections to Current Analysis

3. Claims 1, 2, 4, 6, and 8 are rejected under 35 U.S.C. 102(b) as being anticipated by Richard et al (U.S. Patent 2565990).

4. *"In regards to claim 1, Richard et al disclose a method of controlling an aircraft in a turn without the use of a rudder by producing induced yaw, comprising creating a net induced drag differential between an inboard wing to the turn and an outboard wing to the turn, the net induced drag differential is created in such a manner that the net induced drag differential overcomes adverse yaw produced by the outboard wing (col. 1, lines 18-53). Note that Richard et al disclose manipulating "end-plates" on each wing to induce yaw. Although these "end-plates" do not necessarily increase the effective aspect ratio of the wings, they do create a moment force via an induced drag differential between the inboard and outboard wings.* ***The induced drag is an inherent consequence of allowing stronger wing-tip vortices to form from the bottom of the inboard wing to the top. Note that there is no limitation on the level of adverse yaw produced and it is reasonable to assume that a relatively small aileron deflection will create a comparably small degree of adverse yaw."***

Analysis

Adverse Yaw has many components, and an unfavorable induced drag differentials pointing the aircraft in a direction opposite to the turn has always been considered one of them (Please refer to **Figure 5.** for confirmation). The Method of Induced Yaw's primary concern is changing the *direction* of that induced drag differential from unfavorable to one that is favorable to the turn. *Magnitude* of Induced Yaw produced is a secondary concern.

For the reasons cited in the response to #2 we have shown that for small deflection angles, as referred to in the Examiner's comments, the contribution that the induced drag differential created by Richard's endplates makes to the yaw moment, ***points the aircraft in an unfavorable direction***, for all combinations of endplate deflection angles. In doing so it fails the primary criteria for the Method of Induced Yaw, which is to yaw the wing in an unfavorable direction to the turn.

The Examiner's statement above is made under the (incorrect) assumption that Richard's configuration, as shown in **Fig. 3**, produces a favorable induced drag differential that will overcome *all other forms of adverse yaw* (interference, parasite, etc.). When in reality the exact solution, as presented in the aerodynamic analysis and outlined in response to #2, shows that the direction of the induced drag differential points the aircraft in an unfavorable direction when configured as shown in **Fig. 3**. This will contribute to, and not overcome, adverse yaw at small endplate deflection angles.

5. *In regards to claim 2, Richard et al disclose that the net induced drag differential is produced by controlling the aircraft such that the induced drag experienced by the inboard wing is greater than the induced drag experienced by the outboard wing (see fig. 3 following).* ***Note that the left (inboard) wing "end-plate" is pivoted and the right ("outboard") wing "end-plate" is in a "neutral" position. The pivoted "end-plate" induces greater drag than the "neutral" plate.***

For the reasons cited in response to #2, we have shown that for Richard's design as presented in Fig.3, that the ("outboard") wing "end-plate" in the "neutral" position will produce greater lift and more induced drag than the left (inboard), for all possible deflections of the left endplate that align it in the upward "decreased lift" position (See **Figure 12** for illustration of this result). The end result of this combination is an induced drag differential produced between the inboard and outboard wing points the aircraft in a direction unfavorable to the turn. This is by definition adverse yaw, and is not the "Method of Induced Yaw" as outlined in claim 1.

6. *In regards to claim 4, Richard et al disclose spoiling a tip vortex on the outboard wing to reduce downwash coming off the outboard wing and reduce the induced drag experienced by the outboard wing; and increasing a tip vortex on the inboard wing to increase downwash coming off the inboard wing and increase the induced drag experienced by the inboard wing (col. 1, lines 18-53).* ***Note that the neutrally positioned "end-plate" on the right ("outboard") wing spoils or blocks the wingtip vortex reducing downwash and the pivoted "end-plate" on the left ("inboard") wing allows a wingtip vortex increasing downwash.***

The vortex formation is a component of the multi-step process creating induced drag which to summarize: pressure differential between wing top and bottom drives 3 dimensional flow about wing and wingtips (but is not limited to *just* the wingtips, see **Figures 3 and 4** of this report for confirmation). The net value of the trade-offs between pressure gradient and vortex strength is contained in the estimate of induced drag. Loosely, the wing with the greater induced drag has the higher vortex strength than that with the lesser induced drag.

For the reasons cited in response to # 2 and results shown in **Figures 12 and 13**, we see that the amount of induced drag generated for the endplate when it is deflected upwards to the "decreased lift" position is less than that which is created for the endplate in the "neutral" position. It follows then that the endplate in the "decreased lift" position would be less effective at spoiling or blocking a vortex than the endplate in the "neutral" position.

7. *In regards to claims 6 and 8, Richard et al disclose providing adaptive control surfaces as part of the inboard and outboard wings to* ***form a variable planform to affect the induced drag of each of the inboard and outboard wings and produce the net induced drag differential to overcome adverse yaw produced by the outboard wing*** *(see fig. 3 following). Although figure 3 is a frontal view of the plane,* ***it is clear and inherent that the manipulation of the "end-plates" constitutes a variable planform. As previously stated, the manipulation of the "end-plates' induces the drag differential.***

The manipulation of the endplates does indeed create an induced drag differential, but does so in a manner that produces adverse yaw to the turn. For the reasons cited in response to # 2 and results shown in **Figures 12 and 13**, we have shown that for all combinations of endplate deflections, the wing outboard to the turn will always create more induced drag than the wing inboard to the turn. The result is a net induced drag differential that will create to adverse yaw to the turn, and is not the "Method of Induced Yaw" as outlined in claim 1.

References

1. Hoerner, S. F., "Fluid Dynamic Lift", Hoerner Fluid Dynamics, 1975.
2. Hoerner, S. F., "Fluid Dynamic Drag", Hoerner Fluid Dynamics, 1975.
3. Hemke, P. E., "Drag of Wings With End Plates", NACA Report No. 267, 1927.
4. Mangler, W., "The Lift Distribution of Wings with End Plates", NACA TM-856, April 1938.
5. Riebe, J. M., and Watson, J. M., "The Effect of End Plates on Swept Wings at Low Speed", NACA TN-2229, November 1950.
6. Heyson, H.H, Riebe, G. D., and Fulton, C.L., "Theorectical Parametric Study of the Relative Advantages of Winglets and Wing-Tip Extensions," NASA TP-1020 1977.
7. Maughmer, M. D., "Design of Winglets for High-Performance Sailplanes", *Journal of Aircraft*, Vol. 40, No.6, November-December 2003
8. Hoffstadt, B. A., "Analysis and Design of Winglets for Standard Class Sailplanes", Master of Science Thesis, The Pennsylvania State Universiy, Aerospace Engineering, May 1997.
9. DeYoung, J., "Induced Drag Ideal Efficiency Factor of Arbitrary Lateral-Vertical Wing Forms", NASA Contractor Report 3357, 1980.
10. Cone, C. D., "The Theory of Induced Lift and Minimum Induced Drag of Nonplanar Lifting Systems", NASA Technical Report R-139, 1962.
11. Eppler, R. "Induced Drag and Winglets," *Technical Soaring,* Vol. 20, No. 3, July 1996, pp. 89-96.

12. van Dam, C. P., "Analysis of Non-Planar Wing-Tip-Mounted Lifting Surfaces on Low Speed Airplanes", NASA Contractor Report 3684, June 1983.
13. Anderson, J. D., "Fundamentals of Aerodynamics, 2nd Ed.", 1991.
14. McCormick, B. W., "Aerodynamics, Aeronautics, and Flight Mechanics, 2nd Ed.", 1995.

Appendix

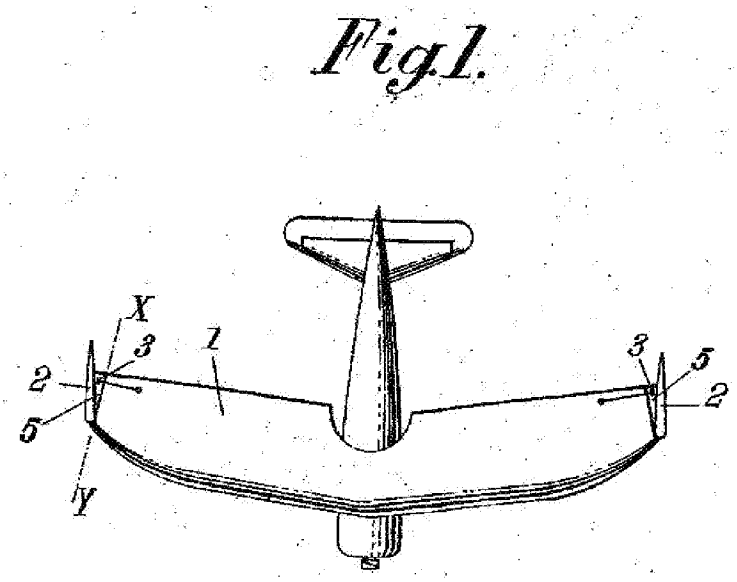

Main Wing

Span = 23.7 L
S = 87.06 L^2
A = 6.45

Ellipse

Height = 5.63 L
Width = 3.5 L
S_E = 15.5 L^2

Measured Hinge Angle = 13° WRT Body Central Axis

Euler Angles Body Fixed – Plate Fixed Orientation, neutral positon
Phi = 0°
Theta = 0°
Psi = 13°

Wing Airfoil: NACA 2414
Endplate Airfoil: NACA 0012

Body Fixed Axes to ECI - The Euler angles ψ, θ, ϕ define rotations that relate the body-fixed coordinates to the ECI system. The rotation sequence from ECI coordinates to body-fixed coordinates (with all rotations in a right-hand sense) is shown in Figure 4:

1.) Rotation by ψ about the Z axis (yaw)
2.) Rotation by θ about the rotated Y axis (pitch)
3.) Rotation by ϕ about the rotated X axis (roll)

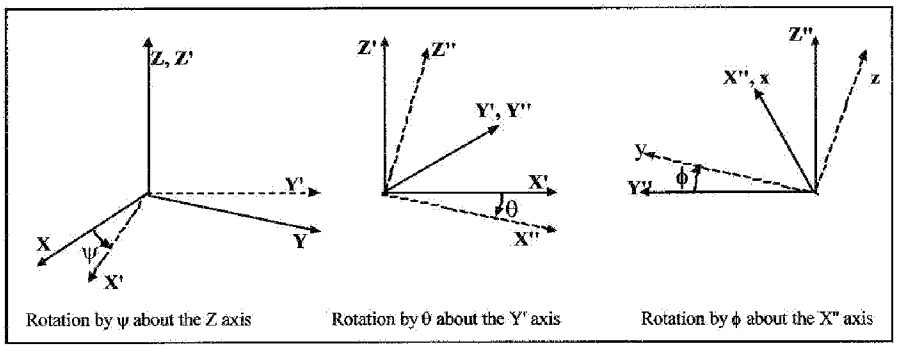

Figure 4. Euler Angles

With this order of rotation, the direction cosines can be defined in terms of the Euler angles as:

$$
\begin{aligned}
\ell_1 &= \cos\psi\ \cos\theta \\
\ell_2 &= \sin\psi\cos\theta \\
\ell_3 &= -\sin\theta \\
m_1 &= \cos\psi\sin\theta\sin\phi - \sin\psi\cos\phi \\
m_2 &= \sin\psi\sin\theta\sin\phi + \cos\psi\cos\phi \\
m_3 &= \cos\theta\sin\phi \\
n_1 &= \cos\psi\sin\theta\cos\phi + \sin\psi\sin\phi \\
n_2 &= \sin\psi\sin\theta\cos\phi - \cos\psi\sin\phi \\
n_3 &= \cos\theta\cos\phi
\end{aligned}
\qquad (3.14)
$$

The inverse transformation can be performed in a number of ways, and the Euler angle set for a given direction cosine matrix is not unique. While not required simulation quantities, they are available as code output. The following inverse transformation was selected:

$$\text{if} \qquad |\ell_3| < 1$$

$$\theta = \sin^{-1}\left(-\ell_3\right) \tag{3.15}$$

$$\phi = \tan^{-1}\left(\frac{m_3}{n_3}\right)$$

$$\psi = \tan^{-1}\left(\frac{\ell_2}{\ell_1}\right)$$

if $\quad |\ell_3| = 1$

$$\theta = \frac{\pi}{2}\frac{\ell_3}{|\ell_3|} \tag{3.16}$$

$$\phi = 0$$

$$\psi = \cos^{-1}\left(m_2\right)$$

Wind Axes – The wind axes coordinate system (x_w, y_w, z_w) is related to the body-fixed coordinates by the angles α and β, as shown in Figure 5. In the wind axes system, x_w is tangent to the flight path (positive forward), z_w is in the vehicle x-z plane (positive downward), and y_w completes the right-hand system.

The body axes (x_b, y_b, z_b) and wind axes (x_w, y_w, z_w) are related by

$$\begin{pmatrix} x_b \\ y_b \\ z_b \end{pmatrix} = [\alpha][\beta]\begin{pmatrix} x_w \\ y_w \\ z_w \end{pmatrix} \tag{3.17}$$

where

$$[\alpha] = \begin{bmatrix} \cos\alpha & 0 & -\sin\alpha \\ 0 & -1 & 0 \\ -\sin\alpha & 0 & -\cos\alpha \end{bmatrix}$$

$$[\beta] = \begin{bmatrix} \cos\beta & -\sin\beta & 0 \\ \sin\beta & \cos\beta & 0 \\ 0 & 0 & 1 \end{bmatrix} \tag{3.18}$$